JOURNAL OF MATERIALS SCIENCE 26 (1991) 2887–2892

Residual stress estimation of a silicon carbide–Kovar joint

TOSHIHIRO YAMADA, MOTOHIRO SATOH, AKIOMI KOHNO, KAZUAKI YOKOI
Mechanical Engineering Research Laboratory, Hitachi Ltd, 502 Kandatsu-machi, Tsuchiura-shi, Ibaraki-ken 300, Japan

Residual stress of silicon carbide and Kovar is calculated using the elasto-plastic method and its validity is checked by the four-point bending test. Silicon carbide and Kovar (Fe–27% Ni–7% Co) are diffusion bonded using Al–10% Si alloy clad on a pure aluminium sheet at 883 K and 4.9 MPa under a vacuum condition. The non-linear structure analysis program (ADINA) is used for the stress estimation. It is found by the calculation that the maximum tensile stress, about 170 MPa, is generated in the silicon carbide close to the interlayer. In the bending test, the fracture of the joint is found to occur from the point where the maximum calculated tensile stress is generated, and the bending strength of the joint is 113 MPa. It becomes clear that the calculated stress and the measured strength of the joint is nearly equal to the strength of the silicon carbide itself (280 MPa). Therefore, it can be concluded that the stress estimation in this method indicates a good approximation of the practical residual stress of the joint.

1. Introduction

There has been considerable progress in recent years in applying ceramics to electronic devices. Recently, silicon carbide has been receiving attention as a new type of ceramic material. Because of its high thermal conductivity, highly effective electronic devices can be designed. However, there are also many problems to be solved in order to construct new effective devices using silicon carbide.

Bonding of silicon carbide and metal is listed as one of the major problems. To add to the bonding processes of ceramics and metals applicable to industry [1], we have developed diffusion bonding using Al–10% Si alloy clad on a pure aluminium sheet as an interlayer. The bonding conditions related to this process to achieve high strength of the joint were also determined [2, 3]. Furthermore, it was found that the Al–10% Si interlayer acted as a stress reliever, as well as a reaction promoter.

It has been shown that the hermetic seal of the joint using this method was strongly influenced by residual stress induced by a thermal expansion mismatch [4]. Therefore, the stress relief of the joint is of prime importance in producing a reliable joint [5–7].

In a previous paper [8], results were obtained from a practical residual stress measurement of an alumina and steel joint. The results showed that the measured practical stress was much lower than the calculated value utilizing the finite element method (FEM) of a fully elastic model, although the tendency of the stress distribution was similar. A more precise estimation of residual stress distribution is required when new ceramics such as silicon carbide and aluminium nitride are applied to electronics devices or machine parts.

In this paper, the residual stress of silicon carbide–Kovar (Fe–27% Ni–7% Co alloy) joints bonded by an Al–10% Si alloy interlayer is estimated by the FEM of an elasto-plastic model. The validity of the estimation will be examined by a bending test of the joint and the silicon carbide itself.

2. Experimental procedure

2.1. Specimen and bonding conditions

Rectangular shaped silicon carbide and Kovar (Fe–27% Ni–7%Co alloy) specimens were used. Fig. 1 shows the specimen size and the combination of the silicon carbide and Kovar. The surface roughness of the specimens is fixed at about $R_{max} = 0.5$ μm by grinding. These specimens are bonded by an Al–10% Si alloy clad on a pure aluminium sheet (the Al–Si interlayer). Details of the Al–Si interlayer are shown in Fig. 2. The thickness of the interlayer is 0.6 mm.

Diffusion bonding was carried out under the conditions given in Table I to obtain the maximum strength of the joint [2, 3]. The physical properties used in the calculation are shown in Table II.

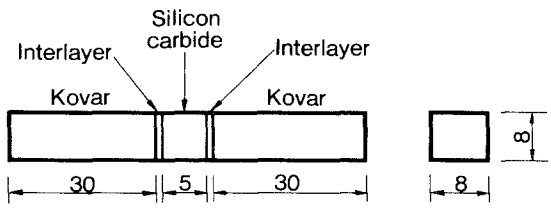

Figure 1 Specimen size and combination. Dimensions in mm.

0022–2461/91 $03.00 + .12 © *1991 Chapman and Hall Ltd.*

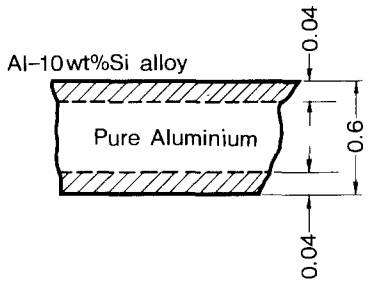

Figure 2 Details of the interlayer. Dimensions in mm.

A four-point bending test of the joints was carried out in order to check the accuracy of the calculation. Spans at the bending test were 18 and 40 mm.

2.2. Calculation of residual stress

An estimation of the residual stress was carried out using a three-dimensional elasto-plastic analysis. A non-linear structure analysis program (ADINA) was applied to the calculation.

TABLE I Bonding conditions

Temperature (K)	Applied pressure (MPa)	Time (ks)	Atmosphere
873	4.9	1.8	Vacuum

The stress of the joint at the bonding temperature (873 K) was assumed to be zero. It was also assumed that the temperature distribution was uniform in the joint when the joint was cooled from the bonding temperature to room temperature, because the cooling rate of the joints was lower than 1.5 °C min^{-1}.

An analysis was performed on the divided model shown in Fig. 3. The origin of the coordinate axes in the model is set in the centre of the silicon carbide. The surface near the interlayer is divided more finely than the other parts of the joint. This is due to the fact that

TABLE II Properties of the materials

Materials	Properties	Temperature (K)				
		293.0	473.0	673.0	723.0	873.0
Kovar	Young's modulus (GPa)	137.2	137.2	137.2	137.2	137.2
	Poisson's ratio	0.3	0.3	0.3	0.3	0.3
	Yield stress (MPa)	431.2	264.6	215.6	205.8	176.4
	Work-hardening factor	130.0	130.0	130.0	130.0	130.0
	Coefficient of thermal expansion (10^{-6} K^{-1})	4.8	4.8	4.8	13.0	13.0
Interlayer (Aluminium)	Young's modulus (GPa)	66.6	61.7	54.9		49.0
	Poisson's ratio	0.3	0.3	0.3		0.3
	Yield stress (MPa)	41.2	29.4	9.8		9.8
	Work-hardening factor	18.0	5.0	1.0		1.0
	Coefficient of thermal expansion (10^{-6} K^{-1})	23.9	24.3	26.5		29.0
Silicon carbide	Young's modulus (GPa)	411.6	411.6	411.6		411.6
	Poisson's ratio	0.27	0.27	0.27		0.27
	Yield stress (MPa)	441.0	441.0	441.0		441.0
	Work-hardening factor	400.0	400.0	400.0		400.0
	Coefficient of thermal expansion (10^{-6} K^{-1})	1.7	3.4	8.4		8.4

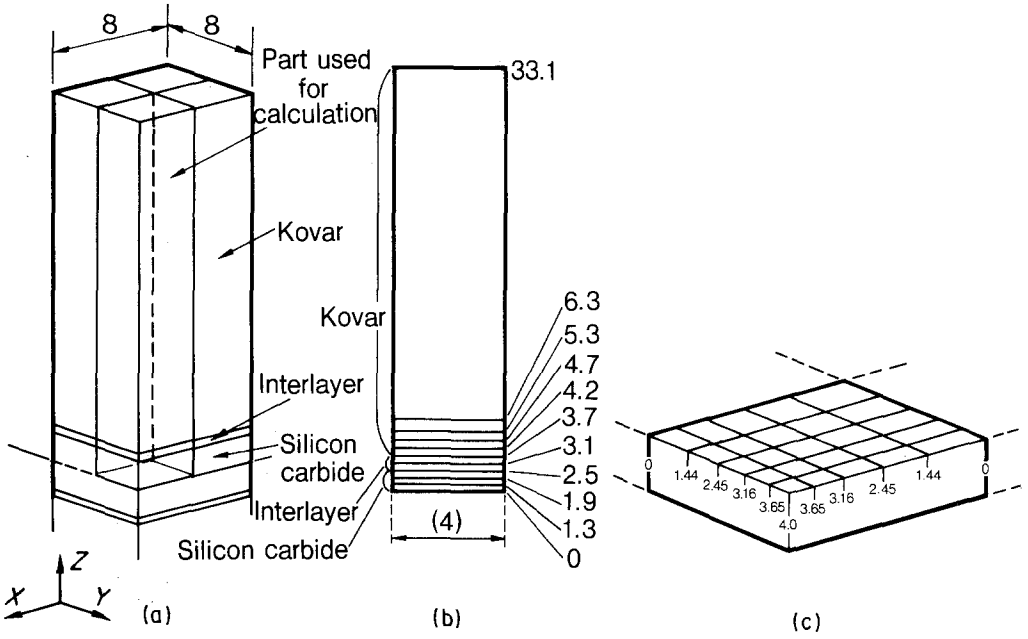

Figure 3 Divided model for the calculation. (a) Outline of the division, (b) division in the Z-direction, (c) division in the X and Y direction. Dimensions in mm.

the maximum tensile stress is generated at the surface of the joint near the interface between the interlayer and the ceramic in the axial direction [8].

In this paper, stress in the axial direction, along which the interface of the joint peels, is mainly discussed because this stress (σ_Z) is considered to influence the strength of the joint.

3. Results and discussion

3.1. Analysis of residual stress by calculation

Distribution of σ_Z in the direction parallel to the joint is shown in Fig. 4. It is shown that the stress near the corner of the joint (0.2 mm from the interface) is about twice that at the centre of the joint and the stress value maximizes on the surface of the joint. This result indicates that the fracture of joints must be initiated on the surface when external stress is applied.

Fig. 5 shows the distribution of σ_Z at (a) the centre and (b) the corner of the joint. In this figure, the maximum tensile stress (approximately 140 MPa) is generated near the interface between the interlayer and the silicon carbide. It decreases abruptly with respect to the distance from the interface between the interlayer and the steel. Comparing the reference points, the stress at the corner of the joint is higher than that at the centre. Furthermore, points where the maximum tensile stress is generated are slightly changed with respect to their reference points. It was found that the maximum tensile stress point is transferred to the silicon carbide side when the tensile stress is increased.

In previous papers [2, 8] we reported that the maximum tensile stress obtained from elastic calculation was about 1000 MPa and was generated in ceramics. When the two calculated values are compared, it is clear that the stress value obtained by the elasto-plastic analysis is much lower than that estimated by the elastic calculation method, although the stress distribution itself is almost similar. The equivalent stress (σ_{eq}), which is determined by interaction between the stress in each direction and the shear stress is also shown in Fig. 5. From the figure, σ_{eq} is a little higher than σ_Z. This result shows that the strength of the joint may be influenced by σ_{eq} rather than σ_Z. Therefore, σ_{eq} is used in the following discussion.

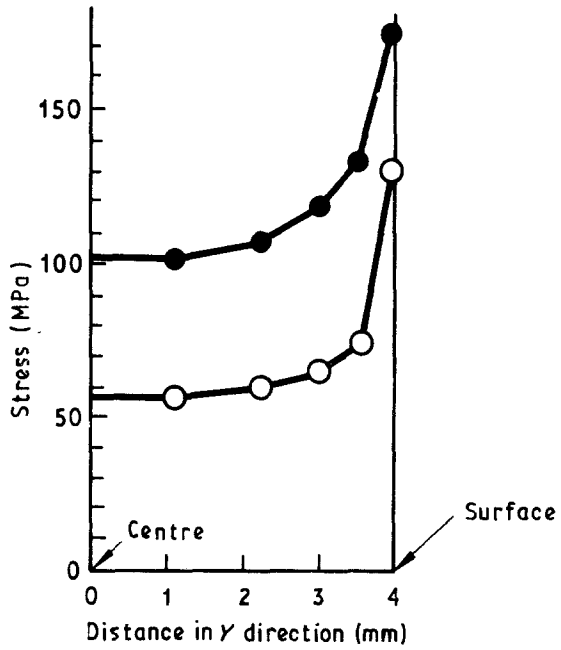

Figure 4 σ_Z distribution in the silicon carbide surface, (●) 0.2 mm from the interface, (○) 0.4 mm from the interface.

From above results, it becomes clear that the maximum tensile stress of the joint (approximately 170 MPa) is generated at the corner of the silicon carbide and the fracture of the joint should initiate from the surface of the silicon carbide at the corner of

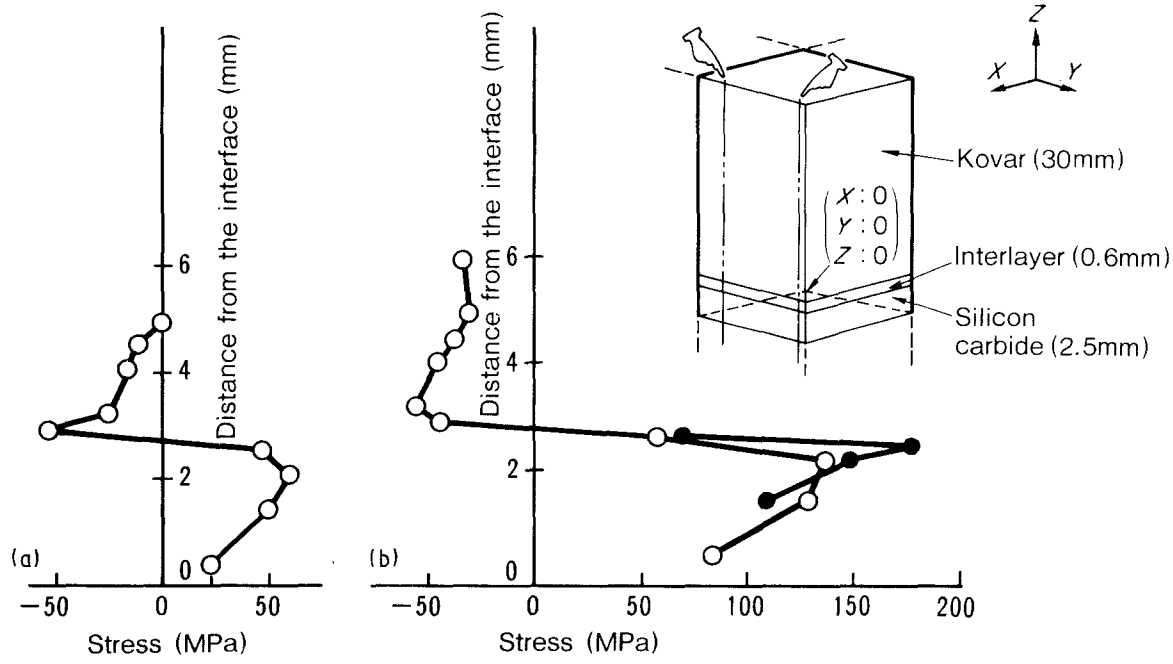

Figure 5 Stress distributions at reference points (a) $X = 3.93$, $Y = 1.14$, and (b) $X = 3.93$ and $Y = 3.93$. (○) σ_Z, (●) σ_{eq}.

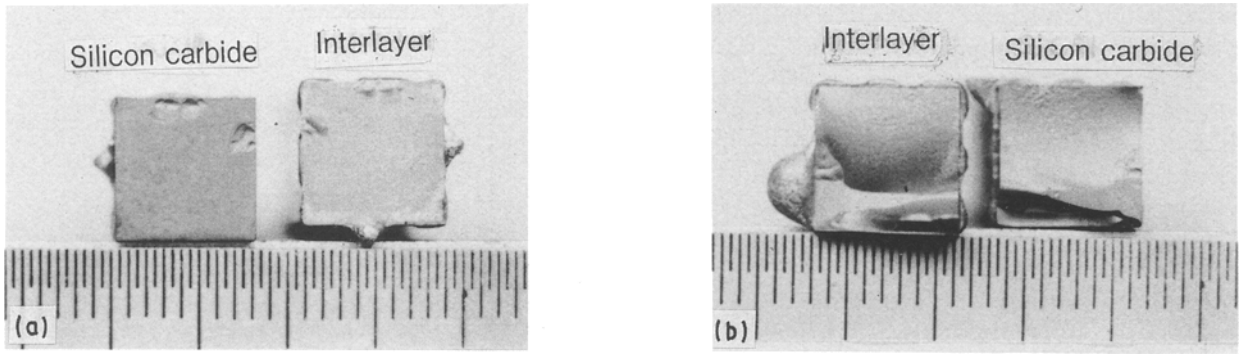

Figure 6 Fractured surfaces of the specimens: (a) interface, (b) Sic.

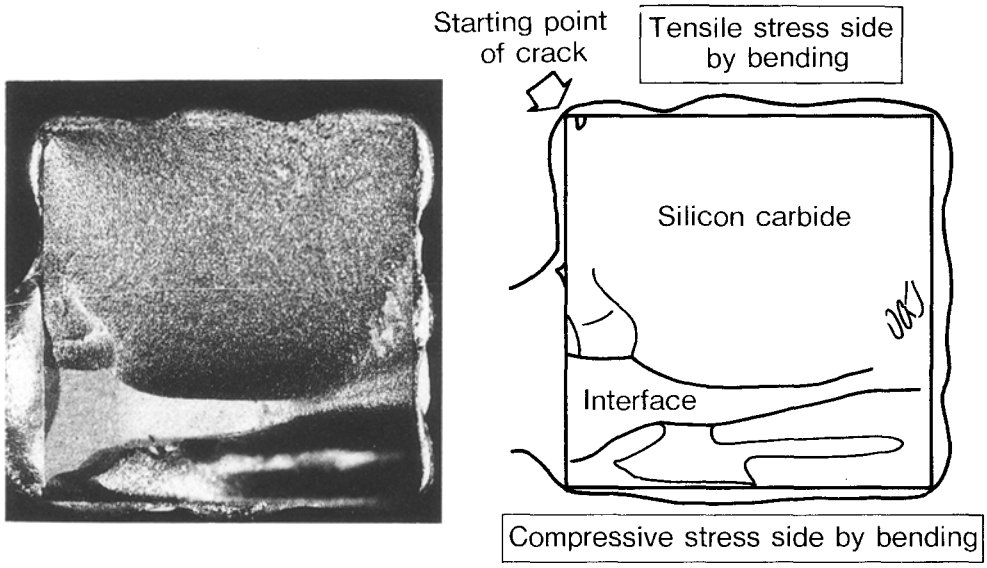

Figure 7 Magnification and schematic drawing of Fig. 6b.

the joint. In the following section, a comparison of the calculated and measured strengths of the joint will be made.

3.2. Bending test of the joint

In order to check the validity of the stress estimation described in the previous section, the bending strength of the joint was measured. Table III shows the strength of the joint using the four-point test and the fracture point. The strength of the joint is varied from 100 to 130 MPa, approximately. The average stress is about 113 MPa. The fracture point of these joints is divided into two types: the silicon carbide, and the interface between the interlayer and the silicon carbide. The ratio of the two types of fracture points is nearly equal but a clear relation between the fracture point and the strength of the joint is not recognized. Typical fractured surfaces of the joint after applying the bending test are shown in Fig. 6. Fig. 6a and b show the fractured surface of the interface and the silicon carbide, respectively. It is clearly seen in Fig. 6b that the silicon carbide was torn off when the fracture occurred. Fig. 7 is a magnification of Fig. 6b. The starting point of the crack is indicated by an arrow in the corner of the joint in the figure. It is clearly shown that the fracture of the joint by the bending test initiates from the surface of the silicon carbide at the corner. This result coincides with the results of the calculation.

TABLE III Strength and fracture points of joints

Bending strength (MPa)	Fracture point
100.9	
108.8	Silicon carbide
112.7	
110.7	Interface between
133.3	interlayer and silicon carbide

Some fractured surfaces were observed by SEM. An example of a surface fractured at the interface between the silicon carbide and the interlayer is shown in Fig. 8. The starting point of the crack, shown by an arrow, is also in the corner of the joint and the crack propagates inward.

It is evident that the torn off silicon carbide remains on the interlayer. In addition, the mass of the silicon carbide which remains on the interlayer increases with increasing distance from the starting point of the initial crack. This result indicates that the strength of the reaction layer between the silicon carbide and the Al–Si interlayer is higher than that of the silicon carbide itself. Fig. 8b–d show the distribution of Al

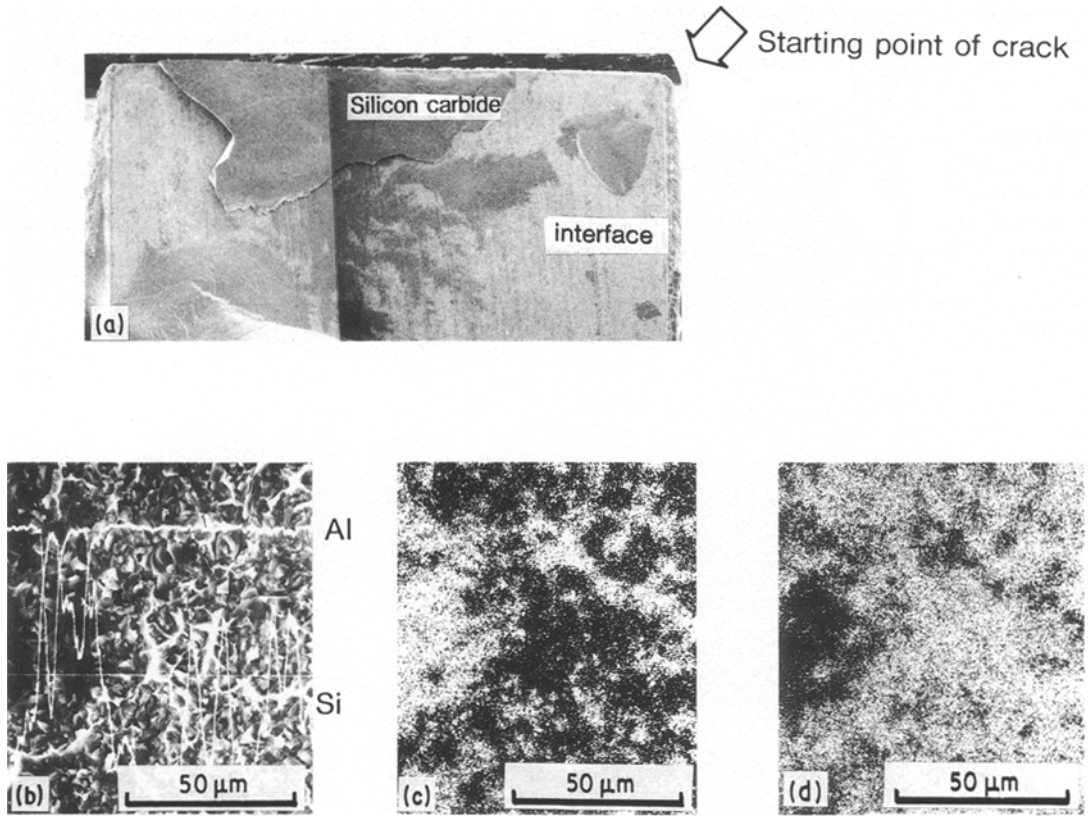

Figure 8 Surface of specimen fractured at the interface between silicon carbide and the interlayer, and distribution of elemental silicon and aluminium, (a) surface of the specimen, (b) intensities of Si and Al X-rays, (c) distribution of Si, (d) distribution of Al.

and Si elements as seen using an X-ray microanalyser (XMA). Al and Si react with each other and diffuse. This conjecture is supported from the results in Fig. 8b–d.

Fracture of materials is usually caused by both external and internal stress, in other words, fracture usually depends on residual stress, unless major defects exist in the material itself. Therefore, it is assumed that the relationship between the bending strength of the joint, σ_b, the residual stress (calculated residual stress, σ_{eq}, in this study) and the bending strength of silicon carbide itself, σ_{SiC}, can be represented by Equation 1 if the calculated residual stress is close to the practical stress

$$\sigma_{eq} + \sigma_b \geqslant \sigma_{SiC} \quad (1)$$

In order to check the strength of the silicon carbide itself, the bending test was carried out using 8 mm × 8 mm × 36 mm specimens. The bending strength of the joint fractured at silicon carbide, σ_b, the calculated residual stress, σ_{eq}, and the bending strength of silicon carbide itself, σ_{SiC}, are summarized in Table IV. As shown in Table IV, the sum of σ_{eq} and σ_b is approximately 280 MPa and the average bending strength of the silicon carbide (σ_{SiC}) is also about 280 MPa. Therefore, it is clear that Equation 1 can be used under these experimental conditions. From the results, it can be concluded that the calculated stress indicates a good approximation of the practical stress.

4. Conclusions

Residual stress of the silicon carbide and Kovar joint was calculated using the elasto-plastic method. The four-point bending test was used to check the effect of residual stress on the strength of the joint.

The results obtained here are summarized below.

1. The strength of the silicon carbide and Kovar using the four-point bending test is approximately 110 MPa. The fracture initiated from the interface between the interlayer and the silicon carbide, or by the silicon carbide itself.

2. The maximum tensile stress is found in the silicon carbide close to the interlayer. The maximum stress is about 170 MPa.

3. By comparing the strength of the silicon carbide, the strength of the joint and the calculated residual stress, it can be concluded that the stress estimation

TABLE IV Comparison of σ_b, σ_{eq} and σ_{SiC}

Bending strength of joint, σ_b (MPa)	Average of σ_b (MPa)	Calculated stress, σ_{eq} (MPa)	Bending strength of silicon carbide, σ_{SiC} (MPa)	$\sigma_b + \sigma_{eq}$ (MPa)
100.9	107.5	171.5	337.1	279.0
108.8			252.8	
112.7			251.9	

used in this method gives a good approximation of the practical stress.

References

1. M. G. NICHOLAS and D. A. MORTIMER, *Mater. Sci. Technol.* **1** (1985) 657.
2. T. YAMADA, A. KOHNO, K. YOKOI, and S. OKADA, "Fundamentals of Diffusion Bonding" (Elsevier, Tokyo, 1987) p. 489.
3. A. KOHNO, T. YAMADA and K. YOKOI, *J. Jpn Inst. Metals* **49** (1985) 876.
4. T. YAMADA, M. HORINO, A. KOHNO, M. SATOH and K. YOKOI, *Welding J.*, to be published.
5. M. G. NICHOLAS and R. M. CRISPIN, *J. Mater. Sci.* **17** (1982) 3347.
6. K. SUGANUMA, T. OKAMOTO, M. KOIZUMI and M. SHIMADA, *J. Amer. Ceram. Soc.* **62** (1984) C256.
7. K. SUGANUMA, T. OKAMOTO and M. KOIZUMI, *ibid.* **68** (1985) C334.
8. T. YAMADA, K. YOKOI and A. KOHNO, *J. Mater. Sci.* **25** (1990) 2188.

Received 30 October 1989
and accepted 30 May 1990